JOURNAL OF AGRICULTURAL AND FOOD CHEMISTRY
60th Anniversary



Article

# Interactions between #-tocopherol and rosmarinic acid and its alkyl esters in emulsions: synergistic, additive or antagonistic effect?

Atikorn Panya, Ketinun Kittipongpittaya, Mickaël Laguerre, Christelle Bayrasy, Jerome Lecomte, Pierre Villeneuve, D. Julian McClements, and Eric A. Decker

*J. Agric. Food Chem.*, **Just Accepted Manuscript** • Publication Date (Web): 18 Sep 2012

# Interactions between α-tocopherol and rosmarinic acid and its alkyl esters in emulsions: synergistic, additive or antagonistic effect?

Atikorn Panya[1], Ketinun Kittipongpittaya[1], Mickaël Laguerre[2], Christelle Bayrasy[2], Jérôme Lecomte[2], Pierre Villeneuve[2], D. Julian McClements[1] AND Eric A. Decker[1*]

[1]Department of Food Science, University of Massachusetts, Chenoweth Laboratory, 100 Holdsworth Way, Amherst, MA 01003, USA; [2]CIRAD, Dept PERSYST, UMR IATE, F-34398 Montpellier 5, France

[*]Corresponding Author

Running Title: Interactions between rosmarinate esters and α-tocopherol in oil-in-water emulsions

## ABSTRACT

Many antioxidants can interact to produce synergistic interactions that can more effectively inhibit lipid oxidation in foods. Esterification of rosmarinic acid produces a variety of compounds with different antioxidant activity due to differences in polarity and thus differences in partitioning in oil, water, and interfacial regions of oil-in-water emulsions (O/W). Therefore, rosmarinic acid and rosmarinate esters provide an interesting tool to study the ability of antioxidant to interact in O/W emulsions. In O/W emulsions, rosmarinic acid (R0) exhibited the strongest synergistic interaction with α-tocopherol while butyl (R4) and dodecyl (R12) rosmarinate esters exhibited small synergistic interaction and eicosyl rosmarinate esters (R20) exhibited slightly antagonistic interaction. Fluorescence quenching and electron paramagnetic resonance (EPR) studies showed that water soluble rosmarinic acid (R0) exhibited more interactions with α-tocopherol than any of the tested esters (R4, R12, R20). This was also confirmed in O/W emulsions where R0 altered the formation of α-tocopherol quinone and α-tocopherol increased the formation of caffeic acid from R0. This formation of caffeic acid was proposed to be responsible of the synergistic activity of R0 and α-tocopherol since the formation of an additional antioxidant could further increase the oxidative stability of the emulsion.

## INTRODUCTION

Under current limitations of approved antioxidants for food applications, it is often challenging for food scientists to maintain the oxidative stability of processed foods. To try to solve this problem, several strategies have been attempted to improve antioxidant performance. One interesting strategy is to use combinations of antioxidants to produce synergistic interactions via free radical transfer mechanisms. For example, the regeneration of oxidized α-tocopherol by ascorbic acid, flavonoids, carotenoids, phospholipids, amino acids and peptides has been reported (*1-7*). These regeneration reactions have been postulated to produce synergistic antioxidant interactions.

Several models to study interactions between antioxidants combinations include the oxygen radical absorbance capacity (ORAC) (*8, 9*), 2,2-diphenyl-1-picrylhydrazyl (DPPH) radical scavenging (*10-14*), ferric reducing antioxidant power (FRAP) (*12*), and homogeneous solutions of peroxidizing methyl linoleate (*15*). Unfortunately, these models often produce inconsistent results. It was reported that the combinations between α-tocopherol and flavonoids exhibit synergistic, additive, and antagonistic effects in the ORAC model (*8, 9*). However, Hiramoto and coworkers (*14*) reported that synergistic antioxidant interactions were observed only when α-tocopherol was combined with ascorbic acid, but not with other water soluble antioxidants in the DPPH model.

The free radical scavenging properties of antioxidants in homogenous model systems (e.g. DPPH and ORAC) might not correlate to foods since foods are heterogeneous (*16*) and thus may have physical attributes not encountered in homogenous systems that can impact antioxidant interactions. For example, the existence of both lipid and aqueous phases would affect antioxidant partitioning and thus interactions between oil and water soluble antioxidants at the oil-water interface. Fukazawa and coworkers reported that interactions between α-

tocopherol and ascorbic acid in liposomal membranes are influenced by physical barriers and surface charge of the membranes (*17*). Currently, there are no systematic methods to be able to predict how combinations of antioxidants can inhibit oxidation in real food systems in a synergistic, additive, or antagonistic manner.

In this research, we hypothesized that antioxidants partitioning at different locations in oil-in-water (O/W) emulsions may influence the ability of antioxidants to interact. Rosmarinic acid and its alkyl esters are excellent tools to study interactions with α-tocopherol because their distributions and locations in O/W emulsions can be varied without impacting on their reactive hydroxyl groups (*18*). In the current study, several methods were utilized to study the interactions between α-tocopherol and rosmarinic acid or its alkyl esters. Electrochemical properties of these phenolic compounds were investigated by cyclic voltammetry (CV) to explain thermodynamic reactions between antioxidants. Direct observations of interactions between rosmarinates, rosmarinic acid, and α-tocopherol were observed by a fluorescence quenching technique. The efficiency of tocopheroxyl radical regeneration by rosmarinic acid and rosmarinate esters was studied by electron paramagnetic resonance (EPR) in homogeneous (ethanol) and heterogeneous (Tween 20 micelles) systems. Finally, the sparing effects of antioxidant interactions between rosmarinate esters, rosmarinic acid, and α-tocopherol during the oxidation of O/W emulsions were investigated by determining the rates of antioxidant decomposition by high-performance liquid chromatography (HPLC). Through these studies, important mechanistic information can be obtained to better predict when synergistic, additive, or antagonistic antioxidant interactions can occur in O/W emulsions.

## MATERIALS AND METHODS

### Chemicals and Materials

Soybean oil was purchased from a local grocery market in Amherst, MA. Ethylenediaminetetraacetic acid (EDTA) disodium salt was purchased from Chempure ™ Ultra (Houston, Texas). Acetic acid, acetonitrile, methanol, hydrochloric acid were obtained from Fisher Scientific (Pittsburgh, PA). Chelex® 100, rosmarinic acid, caffeic acid, 2,2-diphenyl-1-picrylhydrazyl (DPPH), $FeSO_4$, Tween 20™ (Mw ≈1228), $BaCl_2$, $Bu_4$ $NPF_6$, phosphoric acid, sodium phosphate mono- and dibasic, 2,2,6,6-tetramethylpiperidinoxyl (TEMPO) radical were purchased from Sigma-Aldrich (St. Louis, MO). α-Tocopherol quinone was purchased from Tokyo chemical industry (Tokyo, Japan). Double-distilled and deionized water was used for the preparation of all solutions.

### Synthesis of Rosmarinate Esters

The chemoenzymatic esterification of rosmarinic acid to obtain rosmarinate esters was carried out following the procedure described by Lecomte and coworkers (*18*). Briefly, the chemical esterification of rosmarinic acid (56 μmol) was conducted in sealed brown flasks each containing 5 mL of alcohol (methanol, 123.4 mmol; n-butanol, 54.6 mmol; n-octanol, 31.9 mmol; n-dodecanol, 22.5 mmol; n-hexadecanol, 17.0 mmol; n-octadecanol, 15.1 mmol or n-eicosanol, 13.6 mmol). The reaction mixtures were stirred (orbital shaker, 250 rpm, 55-70 $^{o}$C) prior to the addition of the catalyst; the strongly acidic sulfonic resin Amberlite IR-120H (5% w/w, total weight of both substrates) that had been previously dried at 110 $^{o}$C for 48 h. The water generated during the reaction was removed by adding 3 A°, 4-8 mesh molecular sieves (40 mg/mL, Aldrich, St. Louis,MO) to the medium. Samples (20 μL) were regularly withdrawn from the reaction medium and then mixed with 980 μL of methanol,

filtered (0.45 μm syringe filter Millex-FH, Millipore Corp., Bedford, MA), and analyzed by reverse phase HPLC with UV detection at 328 nm (*18*). After complete (4-21 days) conversion of rosmarinic acid into the corresponding ester, the latter was purified in a two-step procedure. First, a liquid-liquid extraction using hexane and acetonitrile was performed to remove the excess alcohol. Then, the remaining traces of the alcohol and rosmarinic acid were eliminated by flash chromatography on a CombiFlash Companion system (Teledyne Isco Inc., Lincoln, NE). Separation was carried out on a silica column using an elution gradient of hexane and ether (20-100% in 35 min). The yield of purified esters, obtained as pale yellow to yellow amorphous powders, was calculated from calibration curves previously established with pure compounds. Pure esters and rosmarinic acid were then fully characterized by ESI-MS, $^{1}$H NMR, and $^{13}$C NMR as previously described by Lecomte et al. (*18*).

**Emulsion Preparation**

Stripped soybean oil was prepared according to the method of Waraho et al. (*19*). The effectiveness of stripping was monitored by measuring the removal of tocopherols by HPLC (*20*). No tocopherol could be detected in the stripped oils. Oil-in-water (O/W) emulsions were prepared using 1.0% (wt) stripped soybean oil in a 10 mM phosphate buffer solution (pH 7.0). Tween 20 was used as an emulsifier at a 1:10 emulsifier/oil ratio. Stripped soybean oil, Tween 20, and phosphate buffer were added to a beaker, and a coarse emulsion was made by blending with a hand-held homogenizer (M133/1281-0, Biospec Products, Inc., Bartlesville, OK) for 2 min. The coarse emulsion was then homogenized with a microfluidizer (Microfluidics, Newton, MA) at a pressure of 9 kbar for three passes.

After the O/W emulsion was prepared, rosmarinic acid and its esters with various chain lengths (4, 8, 12, 18, and 20 carbons) in methanol were added to the emulsion at a final concentration of 30 μM and stirred for 1 h at room temperature. Samples with methanol but without antioxidant were used as control samples. The emulsions (0.5 mL) were transferred into 10 mL GC vials and sealed with (tetrafluoroethylene) butyl rubber septa, and then stored at 25 $^{o}$C in the dark. Three vials of each treatment were taken every day to determine lipid hydroperoxides and hexanal formation.

In some experiments, when needed, emulsions were washed to remove aqueous phase surfactants as previously described by Faraji and coworkers (*21*) with some modifications. In short, emulsions were centrifuged at 38,518 g (17,000 rpm) for 1 h at 4 $^{o}$C using a Fiberlite® F40L-8 x 100 rotor with a high-speed centrifuge (Thermo scientific WX Ultra 80, Asheville, NC). After the centrifugation, the bottom layer (phosphate buffer) was carefully removed using a needle and syringe, and then the same volume of the fresh phosphate buffer was used to re-disperse the creamed emulsion droplet layer by vortexing. This washing procedure was performed a total of three times. The lipid content of the final washed emulsion was determined by the modified Bligh and Dyer method (*22*) and then phosphate buffer was used to adjusted the lipid content back to 1% (w/w). In some experiments, Tween 20 was added back into the washed emulsions (0, 0.1, 0.5, 1.0, and 2.5%; w/w) so that a known amount of surfactant would be in the continuous phase.

**Measurements of particle size of emulsions**

The size of the emulsion droplets were measured by a dynamic light scattering (Zetasizer Nano-ZS, Model ZEN3600, Malvern Instruments, Worchester, U.K.), and expressed as z-average mean diameter. Samples were diluted 50 times with the same buffer as

the emulsion, mixed, and immediately measured by transferring the solution into 3 mL plastic cuvettes for determining the size. Measurements were performed on three replicates and repeated 3 times on each samples at room temperature. The emulsion droplets size ranged from 173.3 ± 11.7 nm and there was no significant change in droplet size of each emulsion over the course of study (data not shown). In addition, there was no visual observation of creaming during storage in all treatments

**Measurements of Lipid Hydroperoxides**

Lipid hydroperoxide formation in emulsion solutions was determined according to the method described by Panya and coworkers (*23*) with some modifications. Emulsion solutions (0.2 mL) were mixed with 1.5 mL of isooctane/2-propanol (3:1 v/v) and vortexed (10 s, three times). After centrifugation at 1000 g for 2 min, 30 μL of the organic solvent phase was mixed with 1.5 mL of methanol/1-butanol (2:1). Hydroperoxide detection was started by the addition of 7.5 μL of 3.94 M ammonium thiocyanate and 7.5 μL of ferrous iron solution (prepared by adding equal amounts of 0.132 M $BaCl_2$ and 0.144 M $FeSO_4$). After 20 min of incubation at room temperature, the absorbance was measured at 510 nm using a UV-Vis spectrophotometer (Genesys 20, Thermo Spectronic). Hydroperoxide concentrations were determined using a standard curve prepared from hydrogen peroxide.

**Measurements of Hexanal**

Headspace hexanal was determined according to the method described by Panya and coworkers (*23*) with some modification using a Shimadzu GC-2014 gas chromatograph (GC) equipped with an AOC-5000 autoinjector (Shimadzu, Tokyo, Japan). A 50/30 μm

divinylbenzene/carboxen/polydimethylsiloxane (DVB/Carboxen/PDMS) stable flex solid phase microextraction (SPME) fiber (Supelco, Bellefonte, PA) was inserted through the vial septum and exposed to the sample headspace for 8 min at 55 $^{o}$C. The SPME fiber was desorbed at 250 $^{o}$C for 3 min in the GC detector at a split ratio of 1:7. The chromatographic separation of volatile aldehydes was performed on a fused-silica capillary column (30 m x 0.32 mm i.d. x 1 μm) coated with 100% poly(dimethylsiloxane) (Equity-1, Supelco). The temperatures of the oven, injector, and flame ionization detector were 65, 250, and 250 $^{o}$C, respectively. Sample run time was 10 min. Concentrations were calculated by using a standard curve made from the above emulsions containing known hexanal concentrations and 200 μM EDTA.

**Calculation of antioxidant interaction indexes of rosmarinate esters and α-tocopherol combinations**

Interaction indexes of rosmarinate esters with α-tocopherol were calculated based on the oxidation lag times of lipid hydroperoxides and hexanal formation. Lag times were determined as the first data point that was statistically ($p \leq 0.05$) greater than time zero. Briefly, the oxidation lag times of individual antioxidants were used to estimate the expected oxidation lag times of its combination. Interaction indexes were calculated from the ratio between the obtained oxidation lag times of the combination and the expected oxidation lag time of the combination with the following equation:

$$\text{Interaction Index} = \frac{\text{Observed lag time of the combination}}{\text{Expected lag time of the combination}} = \frac{Lag\ time\ (control\ A+B) - Lag\ time\ (A+B)}{[Lag time\ (control\ A) - Lag\ time\ (A)] + [Lag time\ (control\ B) - Lag\ time\ (B)]}$$

Where, A and B represent α-tocopherol and rosmarinates, respectively. Controls of A, B and A+B represent the lag time of individuals and combinations without adding antioxidants. Interaction indexes were expressed as synergistic (> 1), additive (≈ 1) and antagonistic (< 1) antioxidant effects

**Determination of Antioxidant Partitioning**

Determination of the physical location of rosmarinic acid and its alkyl esters in the emulsions were performed according to the procedure described by Panya and coworkers (*23*). EDTA (200 μM) was added to regular emulsions and washed O/W emulsions with added surfactants (0, 0.1, 0.5, 1.0, and 2.5%; w/w) to minimize oxidation during analysis. Rosmarinic acid and its alkyl esters in methanol were added to the emulsion at a final concentration of 100 μM followed by stirring at room temperature for 1 h. The emulsions were centrifuged at 162,102 g (46,000 rpm) for 1 h at 4 $^{o}$C using a PTI F65L-6x13.5 rotor with a high-speed centrifuge (Thermo Scientific WX Ultra 80, Asheville, NC). The continuous phase was carefully collected with a pipette and the amount of aqueous phase rosmarinic acid esters was determined directly by HPLC using a modified method described by Lecomte and coworkers (*18*). Briefly, HPLC determination of rosmarinic acid and its alkyl esters was carried out with a Hypersil gold C18 reversed phase column (250 mm x 4.6 mm, 5 μm) equipped with a Hypersil gold guard column (10 mm x 4 mm, 5 μm) (Thermo Scientific, USA) using a LC-10ATvp HPLC system (Shimadzu, USA). Peak integration was performed using Shimadzu EZstart (Version 7.2). Gradient elution was performed using methanol and 3 mM phosphoric acid at 1 mL/min at 40 $^{o}$C (column temperature), in linear gradients from 0/100 (v/v) to 100/0 (v/v) for 5 min, then 100/0 (v/v) for 10 min, back to 0/100 (v/v) for 5 min and hold at 0/100 (v/v) for 5 min. Rosmarinic acid and its alkyl esters [(R4 (4 carbons) – R20

(20 carbons)] were detected with a photodiode array detector (SPD-M10Avp, Shimadzu, USA) at 328 nm. α-Tocopherol was detected at 295 nm. The concentrations of rosmarinic acid esters and α-tocopherol were calculated using a standard curve made from each antioxidant dissolved in methanol.

**Determination of Antioxidant Decomposition during Oxidation Studies**

Determination of the decomposition of α-tocopherol and rosmarinic acid and its alkyl esters in the emulsions during storage were performed according to the procedure described by Panya and coworkers (*23*). A 200 μL sample of O/W emulsions was transferred into 1.5 mL eppendorf tubes containing 50 μL of 200 μM EDTA to inhibit further lipid oxidation. Samples were frozen at -80 $^{o}$C until freezing drying. The freezing drying condition was operated at -10 $^{o}$C for 16 h, then increased the temperature to 5 $^{o}$C for 4 h. Dried emulsions were stored at -80 $^{o}$C until analysis. Antioxidants in dried emulsions were extracted immediately prior to analysis by adding 200 μL of methanol. The mixtures were vortexed for 2 min, sonicated in ultrasonic bath for 2 min, and then centrifuged at 1000 g for 5 min.

The clear methanolic solutions were carefully collected with a pipette and antioxidant concentrations were determined directly by HPLC using a modified method described by Fujimoto and Masuda (*24*). Briefly, HPLC determination of rosmarinic acid and its alkyl esters was carried out with a Hypersil gold C18 reversed phase column (250 mm x 4.6 mm, 5 μm) equipped with a Hypersil gold guard column (10 mm x 4 mm, 5 μm) (Thermo scientific, USA) using a LC-10ATvp HPLC system (Shimadzu, USA). Peak integration was performed using Shimadzu EZstart (Version 7.2). Gradient elution was performed using acetonitrile and 1 % acetic acid at 1 mL/min in linear gradients from 5/95 (v/v) to 100/0 (v/v) for 40 min, then 100/0 (v/v) for 10 min and then back to 5/95 (v/v) for 5 min. Rosmarinic acid and dodecyl

rosmarinate ester (12 carbons) were detected with a photodiode array detector (SPD-M10Avp, Shimadzu, USA) at 328 nm. The oxidation products of rosmarinic acid and its dodecyl ester were detected at 280 and 328 nm. α-Tocopherol and α-tocopheryl quinone were detected at 295 and 265 nm, respectively. The concentrations of antioxidants (rosmarinic acid and its ester, α-tocopherol, and α-tocopheryl quinone) were calculated using a standard curve made from the standard antioxidants dissolved in methanol.

**Front-Face Fluorescence Quenching Measurements**

Front-face fluorescence quenching between α-tocopherol and rosmarinic acid, and its alkyl esters in O/W emulsions was determined by steady-state emission measurements recorded with a PTI spectrofluorometer (PTI, London, Ontario, Canada). Stripped soybean oil (1 %; w/w) emulsions were prepared with 0.1 % (w/w) Tween 20 in 10 mM phosphate buffer (pH 7) with 200 μM EDTA to minimize oxidation. A final concentration of 100 μM of α-tocopherol was added to the O/W emulsions from the stock solution of α-tocopherol in methanol. The mixtures were stirred at room temperature for 1 hour. Then, rosmarinate esters in methanol were transferred into the emulsions containing α-tocopherol at concentrations of 0, 5, 10, 25, 50, and 100 μM.

After vortexing for 2 min, the final emulsions (1.5 mL) were transferred into triangular suprasil cuvettes. The samples were held at 30 $^{o}$C and stirred with a 3 mm magnetic stirring bar (Fisher scientific, USA). Emission was observed at 90$^{o}$ to the incident beam, that is, 22.5$^{o}$ with respect to the illuminated cell surface. The emission of α-tocopherol was measured at 320 nm using an excitation wavelength of 295 nm. Spectral bandwidth for both excitation and emission slits was 2.0 nm, integration time was 1 s, and the wavelength increment was 2.5 nm. The intensity of the spectra (I) of α-tocopherol after addition of the rosmarinate

derivatives was determined as the emission signal intensity (counts per second) measured by means of a photomultiplier. The intensity ratio ($I_o/I$), where $I_o$ is the fluorescence intensity of α-tocopherol, was plotted versus the concentrations of rosmarinate esters. The slope of this line was used to determine the quenching constant of the different rosmarinate esters.

**Cyclic Voltammetry (CV) Measurements**

Cyclic voltammetry was performed according to the method described by Wilson and coworkers (*25*). Rosmarinic acid and its alkyl esters (2 mM) were freshly dissolved in acetonitrile and evaluated with a BASi Model C-3 cell stand using a planar 1 mm diameter glassy carbon working electrode, Ag/AgCl reference electrode, and a Pt wire auxiliary electrode. Samples were scanned at 100 mV $s^{-1}$ at 25 $^{o}$C in acetonitrile with 0.5 M $Bu_4$ $NPF_6$ as a salt bridge in 50 mM phosphate buffer, pH 7 or in 1% Tween 20 in 50 mM phosphate buffer, pH 7.

**Measurement of α-Tocopherol Regeneration by Electron Paramagnetic Resonance Spectroscopy**

The efficiency of rosmarinic acid and its alkyl esters to regenerate α-tocopherol from α-tocopheroxyl radicals was determined by electron paramagnetic resonance (EPR) spectroscopy in two different systems: a homogeneous ethanolic solution and a heterogeneous Tween 20 micelle solution. The experiment procedure was adapted from the method described by Pazos and coworkers (*26*) with some modifications.

For experiments in homogeneous environments, stock solutions of α-tocopherol (2 mM), DPPH radical (0.5 mM), and rosmarinates were prepared freshly with $N_2$ saturated ethanol. In heterogeneous environments, a stock solution of α-tocopherol (2 mM) was

prepared in 100 mM Tween 20 in $N_2$ saturated 50 mM phosphate buffer solution at pH 7. Two mL of the stock solution of α-tocopherol (ethanolic or Tween 20 solutions) was transferred into a 4 mL vial which was purged with $N_2$. Then, 50 μL of the DPPH solution was transferred into the stock solution of α-tocopherol, and mixed immediately at room temperature. After reacting for 20 sec to form α-tocopheroxyl radicals, 50 μL of the stock solutions of rosmarinic acid and its alkyl esters were added and mixed. The final concentrations of α-tocopherol and DPPH were 1.9 and 0.01 mM, respectively. The final concentrations rosmarinic acid and rosmarinates were ranged from 2.5 to 20 μM. All solutions were transferred into an EPR spectrometer via a 5 mL syringe. EPR spectra were recorded 1 min after the reaction with DPPH.

The experiments were performed using a Bruker ELEXSYS E-500 EPR spectrometer (Bruker, Germany) equipped with an X-band microwave bridge and an ER 4122-SHQE high sensitivity single cavity. Samples were injected into the cavity through with Aqua-X flow-through cell. EPR parameters were at the following setting: microwave power, 10 dB; sweep width, 100 G; sweep time, 20.9 s; modulation amplitude, 3 G; time constant, 81.92 ms; receiver gain, 80 dB. All samples were handled under $N_2$ sealed environment at room temperature.

The Mn (II) marker attached with the Aqua-X-flow cell was used to determine the relative signal intensity of the α-tocopheroxyl radical (the peak-to-peak ratio between α-tocopheroxyl radical and the marker). Concentrations of α-tocopheroxyl radical were quantitated by comparing the double-integrated areas of α-tocopheroxyl radical to known concentration of TEMPO radical. The integration of the signal was performed by using Bruker Xepr software. Efficiencies of the regeneration of α-tocopherol by each rosmarinates were estimated from the slopes of α-tocopheroxyl radical reduction at various concentrations of rosmarinates.

317 **Statistical Analysis**

318 All analyses were performed on triplicate samples. Oxidation lag phases were defined
319 as the first data point significantly greater than the 0 time value. In all cases, comparisons of
320 the means were performed using Duncan's multiple-range tests. A significance level of
321 $p<0.05$ was defined as being statistically different. All calculations were performed using
322 SPSS17 (http://www.spss.com; SPSS Inc., Chicago, IL).

323

## RESULTS AND DISCUSSION

### Antioxidant Activity of Rosmarinic Acid and its Esters and α-Tocopherol Combinations in Stripped Soybean O/W Emulsions

The ability of rosmarinic acid and rosmarinate esters and α-tocopherol to synergistically inhibit lipid oxidation in the O/W emulsions was tested with rosmarinic acid (R0) and its different esters (R4, R12, and R20). This system was used since the different forms of rosmarinate could primarily exist in the aqueous phase, the interfacial layer, or the emulsion droplet core and thus could interact differently with α-tocopherol (T) which would mainly associate with the oil-water interface and/or the emulsions droplet core. Lipid hydroperoxide and hexanal formation in the O/W emulsions were determined during storage at 25 $^{o}$C in the dark. All forms of rosmarinic acid and its esters (30 μM) were able to inhibit the formation of lipid hydroperoxides and hexanal compared to the control (Figure 1). For example, the R4 was slightly better than R12 at increasing hexanal lag times and R0 was slightly better than R20 which is the worst antioxidant. This antioxidant efficiency order (R4>R12>>R0>R20) confirms the cut-off effect we already observed in O/W emulsion with rosmarinate derivatives (*27, 28*) and chlorogenate alkyl esters (*29*).

All the combinations of rosmarinic acid and its esters (30 μM) with α-tocopherol (30 μM) exhibited better antioxidant activity compared to the individual compounds. This was not entirely unexpected since the total antioxidant concentrations were higher. As shown in Figure 2, it was noted that the combinations of α-tocopherol and butyl rosmarinate ester (T-R4), and α-tocopherol and dodecyl rosmarinate ester (T-R12) exhibited similar increases in the lag phase of lipid hydroperoxides and hexanal formation as the sum of the individual antioxidants (Figure 1). Surprisingly, the combination of α-tocopherol and rosmarinic acid (T-

R0) showed significant increases in the lag phase of lipid hydroperoxides and hexanal formation compared to the sum of antioxidants analyzed individually (synergistic effect). The lag times of hexanal formation and lipid hydroperoxides for the T-R0 combination ended up being similar to the lag times of the T-R4 and T-R12 combinations. In this case, the strong synergistic effect between α-tocopherol and R0 compensates for the much lower antioxidant activity of R0 taken individually compared to R4 and R12. Finally, it clearly appears from Figure 2 that the combination between R20 and α-tocopherol produces an antagonistic effect.

To quantitate the effects of the antioxidant combinations, the lag times for the formation of lipid hydroperoxides and hexanal for both individual and combined antioxidants were used to calculate the interaction index. As illustrated in Figure 3, R0 had the strongest antioxidant synergy with α-tocopherol producing interaction indexes for lipid hydroperoxides and hexanal formation of 4 to 5, while the interaction indexes of α-tocopherol and R4 or R12 were approximately 1.5 to 2 meaning that the synergistic effects were smaller. In contrast, R20 showed significant antagonistic effect with α-tocopherol exhibiting an interaction index of 0.3 to 0.6.

**Partitioning of Rosmarinic Acid, Rosmarinate Esters, and α-Tocopherol in O/W Emulsions**

A factor that could be important for the observed variations in synergistic antioxidant interactions would be differences in the physical location of rosmarinic acid and rosmarinate esters which would impact their ability to interact with α-tocopherol. The aqueous phase of O/W emulsions was collected to determine whether the antioxidants partitioned into the aqueous or emulsion droplet phases (interface + droplet core). Results showed that rosmarinic acid (R0) had the lowest association with emulsion droplets, partitioning at approximately 90

372 % in aqueous phase, while butyl (R4) and dodecyl (R12) rosmarinate esters and α-tocopherol
373 were highly associated with the emulsion droplets indicated by low concentrations (2-9%) in
374 aqueous phase (Figure 4). The antioxidant partitioning of R4, R12 and R20 were consistent
375 with our previous report (*28*). There was slight precipitation observed in the continuous phase
376 of emulsions containing R20. According to our previous study, R20 may form poorly soluble
377 self-assembled aggregates and/or co-micelles with Tween 20 in the aqueous phase (*27, 28*).

378

379 **Interactions between Antioxidants in O/W Emulsions as Determined by Front-Face**
380 **Fluorescence Quenching Measurements**

381 Just because antioxidants partition into the continuous phase or the emulsion droplet
382 does not mean they will interact to produce synergistic or antagonist interactions. Direct
383 observations of the rosmarinic acid or rosmarinate esters interacting with α-tocopherol in O/W
384 emulsions can be determined by quenching of α-tocopherol fluorescence by the rosmarinates.
385 Although the exact quenching mechanisms between these antioxidants have not been
386 reported, one potential mechanism might be Förster resonance energy transfer (FRET)
387 because the emission wavelength of α-tocopherol (325 nm) overlaps with the excitation
388 wavelength (323 nm) of the rosmarinate esters and rosmarinic acid. Therefore, closer the
389 proximity between α-tocopherol and the rosmarinates or rosmarinic acid would be expected to
390 produce greater quenching.

391 In the O/W emulsions, the fluorescence intensity of α-tocopherol was decreased in the
392 presence of butyl and dodecyl rosmarinates and rosmarinic acid. As illustrated in Figure 5, R0
393 was more effective at quenching the α-tocopherol fluorescence in O/W emulsion compared to
394 the rosmarinate esters (R4 to R12) as shown by R0's higher quenching constant. Results
395 suggest that the more water soluble rosmarinic acid (R0) was able to interact with α-

tocopherol on the emulsion droplet surface. The lower the quenching constants of rosmarinate alkyl esters suggest that slow lateral diffusion on the droplet surface would limit their ability to interact with α-tocopherol. This slowing down of the rosmarinate diffusivity may be due to hydrophobic interactions between their alkyl chains and the aliphatic tails of surfactants and lipids at the interface and/or in the droplet interior.

When O/W emulsions are produced, excess surfactant that is not absorbed onto the emulsion droplet surface partitions into the aqueous phase and forms micelles. These micelles can alter the partitioning of antioxidants into the continuous phase by solubilizing the antioxidants into the micelles. To eliminate the influence of surfactant micelles, the excess surfactants in O/W emulsions were removed by a washing process (*28*). Removal of the surfactant micelles decreased the ability of all the rosmarinic acid derivatives to quench the fluorescence of α-tocopherol with the exception of the R4 ester. This decrease was most dramatic for rosmarinic acid (R0) such that its quenching constant became similar to the rosmarinic acid esters (R8, R12). This suggests that the removal of the surfactant micelles decreased the partitioning of α-tocopherol into the aqueous phase which decreased the ability of α-tocopherol and water-soluble rosmarinic acid to interact. The α-tocopherol quenching constants of the other rosmarinate esters also decreased in washed emulsions, suggesting that the Tween 20 micelles also decreased their ability to interact with α-tocopherol. Since all of the antioxidants can partly partition into the interface, the decrease in interfacial area caused by the removal of the micelles would be expected to decrease the partitioning of the antioxidants in the interface of the emulsion droplets and micelles and thus decrease antioxidant interactions especially if some of the antioxidant was forced into the interior of the emulsion droplet.

420

421 **Electrochemical Properties of Rosmarinic Acid, Rosmarinate Esters and α-Tocopherol**

422 One possible reason for the observed variations in antioxidant activity for
423 combinations of rosmarinic acid esters and α-tocopherol could be due to the regeneration of
424 one antioxidant by the other. The hierarchy of antioxidant regeneration by electron transfer
425 can be estimated by their oxidation-reduction potentials. Generally, an antioxidant with lower
426 reduction potential is thermodynamically preferred to give electrons to an antioxidant with
427 higher reduction potential (*30*). Cyclic voltammetry can be a useful method for studying the
428 reduction potential of antioxidant compounds (*31-35*). In this study, cyclic voltammetry was
429 performed in order to measure the electrochemical potential of α-tocopherol and also to
430 investigate the influence of esterification on the electrochemical properties of rosmarinic acid
431 in various solutions.

432 Results showed that cyclic voltammograms of the rosmarinate esters and α-tocopherol
433 exhibited one anodic and one cathodic peak (data not shown) in acetonitrile. This is also true
434 for other phenolic compounds (*36, 37*). As shown in Table 1, all the rosmarinate esters
435 showed a similar oxidation peak ($E_{Pa}^{ox}$) at approximately 1115-1137 mV (vs. Ag/AgCl) in
436 acetonitrile solution which was significantly higher than α-tocopherol (634.9 mV).
437 Electrochemical parameters of the rosmarinate esters did not show the non-linear behaviors
438 that were observed when their activity was tested with the DPPH assay or in lipid oxidation
439 studies (*27-29, 38*).

440 Oxidation peak potentials of rosmarinic acid and α-tocopherol were further studied in
441 50 mM phosphate buffer, pH 7.0 and 1% Tween 20 in 50 mM phosphate buffer solutions.
442 Trolox was used instead of α-tocopherol in these experiments due to solubility limitations of
443 α-tocopherol in aqueous solutions. Results showed that rosmarinic acid reduction potential

444 decreased in the phosphate buffer, however, rosmarinic acid still had higher reduction
445 potentials than Trolox. This was also true in the presence of Tween 20 micelles where the
446 rosmarinic acid reduction potential decreased compared to acetonitrile but was still greater
447 than α-tocopherol. These results suggested that α-tocopherol is thermodynamically preferred
448 to donate electrons to rosmarinic acid.

449

450 **Regeneration Efficiency of the Rosmarinic Acid Esters to Reduce α-Tocopheroxyl**
451 **Radical in Homogeneous and Heterogeneous Systems**

452 The ability of rosmarinic acid and its esters and α-tocopherol to regenerate each
453 other's radicals can be determined by electron paramagnetic resonance (EPR) technique. To
454 determine these interactions, antioxidant radicals were produced by exposing the antioxidants
455 to DPPH radicals. However, rosmarinic acid and its esters were not able to produce stable
456 radicals that could be observed by electron paramagnetic resonance (EPR) using this method,
457 so the following studies focused on the fate of α-tocopherol radicals in the presence of
458 rosmarinic acid and its esters. Experiments were performed in both ethanol and 100 mM
459 Tween 20 solutions in order to observe the ability of the different alkyl chain lengths of
460 rosmarinic acid to impact the efficiency of α-tocopherol regeneration in homogenous and
461 heterogeneous systems. Overall, the efficiency of rosmarinic acid and its esters to reduce α-
462 tocopherol radical was very low as predicted by electron reduction potential (Table 1). The
463 range of α-tocopherol radical regeneration efficiencies by rosmarinic acid and its esters
464 ranged from 0.08 to 0.55 moles α-tocopherol radicals reduced/ mole of phenolics (Figure 6).

465 As shown in Figure 6, esterification of rosmarinic acid increased electron-donating
466 ability towards α-tocopheroxyl radicals compared to rosmarinic acid in ethanolic solutions.

467 Esterification has also been observed to increase the DPPH scavenging activity of rosmarinic
468 acid esters (*18, 28*) and chlorogenic acid esters (*39*) in methanolic solution. Lecomte and
469 coworkers (*18*) reported that dodecyl rosmarinate (R12) had the greatest DPPH scavenging
470 activity of all the esters tested (4-20 carbons), while Lopez-Giraldo and coworkers (2009)
471 showed that butyl and octyl chlorogenate esters had higher DPPH scavenging activity than
472 chlorogenic acid itself and its esters with alkyl chains longer than 12 carbons. In this study,
473 R4 had the highest ability to regenerate the α-tocopheroxyl radical scavenging efficiency
474 compared to other esters in ethanol solution.

475 To investigate the influence of physical structures on α-tocopherol radical
476 regeneration by the rosmarinates, measurements were also performed in 50 mM phosphate
477 buffer solution with surfactant micelles produced from 100 mM Tween 20, pH 7.0. The ratio
478 of scavenging regeneration efficiency in Tween 20 versus ethanol for R0 and R4 increased by
479 381 and 214 %, respectively while R12 and R20 where essentially the same in ethanol and
480 Tween 20. The results for R0 are similar to those observed for R0 quenching of fluorescence
481 again suggesting that the high partitioning of R0 in the aqueous phase allowed it to interact
482 with α-tocopherol radicals at the Tween 20 micelle interface. The fact that R4 was effective at
483 interacting with α-tocopheroxyl radicals but did not alter α-tocopherol fluorescence could be
484 due to the lack of emulsion droplets in the EPR study. The presence of emulsion droplets in
485 the fluorescence study could result in R4 partitioning in the emulsion droplet in a manner
486 where it did not readily interact with α-tocopherol whereas R4 would interact with α-
487 tocopheroxyl radicals in surfactant micelles.

488

489

490

**Depletion of α-Tocopherol, Rosmarinic Acid, and its alkyl Esters during oxidation of O/W emulsion**

Studies on α-tocopherol fluorescence quenching indicated that of all the tested polyphenols, R0 interacted with α-tocopherol more than the rosmarinate esters. This suggests that the ability of α-tocopherol to greatly increase the antioxidant activity of R0 could be due to their molecular interactions. To further investigate the potential interaction between the rosmarinates and α-tocopherol, decomposition of the antioxidants was determined during storage and compared to formation of the lipid oxidation product, hexanal in the O/W emulsion.

The decomposition of R0, R12 and α-tocopherol analyzed individually in the O/W emulsion and subsequent hexanal formation are shown in Figure 7A-C. Results showed that α-tocopherol concentrations decreased in a linear fashion (Figure 7A). α-Tocopherol concentrations were approximately 8-12 μM when the lag phase of hexanal formation ended. The concentration of R0 and R12 also decreased in a linear fashion during storage of the O/W emulsions (Figure 7Band C). However, both R0 and R12 were completely depleted prior to formation of hexanal.

Depletion of R0, R12, and α-tocopherol during the storage of the O/W emulsions when the antioxidants were added in combination is shown in Figure 8 and 9. In this study, α-tocopherol concentration was constant at 30 μM while R0 and R12 concentrations ranged from 15 to 60 μM. As was previously observed in Figures 3, the combination of α-tocopherol and R0 produced synergistic antioxidant activity, while α-tocopherol and R12 showed an additive effect.

513 The decomposition disappearance of R0 and R12 was very similar in the presence of
514 α-tocopherol (Figure 8A and 9 A). For example, the time at which approximately 50% of R0
515 and R12 was lost was about 9 days. The similarity of R0 and R12 depletion in the presence of
516 α-tocopherol suggests that the increase in the antioxidant activity of R0 by α-tocopherol was
517 not due to α-tocopherol regenerating R0 and keeping R0 concentrations higher. Conversely,
518 α-tocopherol depletion was much faster in the presence of R0 than R12 (Figure 8B and Figure
519 9B). For example at 30 days of storage, α-tocopherol concentrations were less than 5 μM in
520 the presence of R0 (60 μM) compared to 11 μM in the presence of R12 (60 μM). In addition,
521 the lag times of tocopheryl quinone (TQ) formation were different between R0 and R12
522 samples (Figure 8B and 9B). For example, tocopheryl quinone was detected in the R0
523 samples when R0 was almost depleted whereas tocopheryl quinone was detected much earlier
524 during storage in the presence of R12 with the lag phase for TQ formation being independent
525 of R12 concentration.

526 The observation that R0 and α-tocopherol samples increased the lag phase for TQ
527 formation and improved their oxidative stability similar to R12 and α-tocopherol samples
528 suggests that the two antioxidants were interacting. Even though the concentrations of α-
529 tocopherol in the combination with R0 were lower than that observed in R12 and α-tocopherol
530 samples, antioxidant activity was greater. This suggests that other antioxidative compounds
531 might exist in the emulsions since it has been reported that some antioxidants can produce
532 other antioxidative compounds via their oxidative degradation (*24, 40*).

533

534 The major oxidation products generated from R0 and R12 were analyzed to get a
535 better understanding of the dynamics of the antioxidant mechanisms in the O/W emulsions.
536 Only one major breakdown product of R0 was observed during storage while two major

breakdown products were observed for R12. From LC-MS analysis, the products at HPLC retention times of 10.5 (in R0 and R12) and 35.9 (in R12) min are caffeic acid [m/z = 179.2 $(M-H)^-$] and a dodecyl rosmarinate quinone formed on the 2-oxyphenylpropanyl moiety [m/z = 525.06 $(M-H)^-$]. The structures of major antioxidant oxidation products were showed in Figure 10. The quinone was previously reported to be the major oxidation product of rosmarinic acid as determined in 2,2-azobis(isobutyronitrile)(AIBN)-induced oxidation of ethyl linoleate and DPPH model systems(*24*).

However, unlike the above single phase model systems using ethyl linoleate and alcohols, our results indicated that the antioxidant product of R0 in O/W emulsions was mainly caffeic acid (Figure 11). This could be because the R0 quinone was unstable in O/W emulsions and was fragmented to caffeic acid. It was reported that rosmarinic acid can be decomposed into caffeic acid via a McLafferty rearrangement (γ-H rearrangement with β-cleavage in the electron ionization) in mass spectrometry analysis (*40*). Caffeic acid has also been found to be one of the metabolites of rosmarinic acid in rats (*41*). Hydrolysis of rosmarinic acid by esterases into caffeic acid and 3,4-dihydroxyphenyllactic acid *in vitro* was reported, however the hydrolysis was not observed in a gastrointestinal model with lipase and pancreatic enzymes (*42*).

In our conditions, however, hydrolysis is unlikely. Instead, an oxidation breakdown is possible on the tertiary carbon (circled carbon on Figure 10) which represents, by far, the most oxidizable carbon due to the three electron-withdrawing effects exerted by the ester, the acid, and the quinone groups. Such position could be oxidized twice which would provoke the scission of the ester bond to produce caffeic acid (Figure 10).

In both the absence and presence of α-tocopherol, caffeic acid was produced from both R0 and R12 (Figure 11). More caffeic acid was produced from R0 in the presence of α-

561 tocopherol (Figure 11A) suggesting that α-tocopherol could be involved in the formation of
562 caffeic acid. The same was true with the case of R12, however, the production of caffeic acid
563 by α-tocopherol was found to a much lower (Figure 11B).

564 In all treatments, caffeic acid was detected at the beginning of the oxidation process
565 and then decreased at the end of the oxidation lag times (Figure 11A and B). Except for R0
566 alone, the hexanal lag times ended before all caffeic acid was depleted. Caffeic acid has the
567 ability to scavenge free radicals (*46*) and Chen and Ho (*47*) reported that caffeic acid had
568 better antioxidant activity in O/W emulsions than rosmarinic acid and α-tocopherol. In this
569 study, the degradation of caffeic acid prior to the end of the lag phase also suggests that it is
570 being preferentially oxidized prior to the fatty acids and thus is acting as an antioxidant.
571 Therefore, the formation of caffeic acid from R0 in the presence of α-tocopherol could
572 explain why this combination had much better antioxidant activity that the individual
573 antioxidants since the caffeic acid would provide an additional antioxidant to slow down
574 oxidation (Figure 10A). In addition to the formation of caffeic acid might be driven by the
575 proximity between R0 and α-tocopherol, it might be enhanced by π-π aromatic interactions
576 between phenolic compounds. It was suggested that the formation of a stable complex
577 between antioxidant due to π-π stacking between the aromatic rings of phenolic compounds
578 may influence on the overall electron donating capacity, resulting synergistic effects (*43-45*).

579 A quinone of dodecyl rosmarinate ester was observed with R12 but not R0 suggesting
580 that the esterification of rosmarinic acid with an alkyl chain can increase the stability of the
581 quinone (Figure 11C) and can thus defavor the formation of caffeic acid. Steric hindrance
582 exerted by the dodecyl chain of the R12 quinone may slow the rosmarinic acid oxidation
583 reactions which produces caffeic acid. Therefore, unlike the extremely reactive R0 quinone

584 which is rapidly converted into caffeic acid, the R12 quinone may exist long enough to be
585 detected.

586 If we consider that α-tocopherol promote the breakdown of the quinone into caffeic
587 acid, the lower concentration of caffeic acid with R12 compared to R0 could also be due to
588 R12 reacting less with α-tocopherol than R0 as shown by the fluorescence and EPR data
589 (Figures 5 and 6) thus decreasing the conversion of the quinone to caffeic acid.

590 Fluorescence quenching results demonstrates that R12 interacts in a much lesser extent
591 than R0 with α-tocopherol. In absence of bimolecular complex, consequently, the R12
592 quinone may be too far from the hydroxyl radicals generated by α-tocopherol. In these
593 conditions, α-tocopherol does not promote any conversion of R12 quinone into caffeic acid,
594 which is the observation made on Figure 11B. Furthermore, this could explain why R12 does
595 not affect the depletion rate of α-tocopherol during the first days (Figure 9B).

596 In conclusion, R0 was physically able to interact with α-tocopherol in surfactant
597 micelles and O/W emulsions. We hypothesize that the observed synergistic antioxidant
598 activity of the combination of R0 and α-tocopherol were not due to the regeneration of α-
599 tocopherol by rosmarinic acid due to the thermodynamic infeasibility of this reaction and the
600 fact that α-tocopherol degradation rates in O/W emulsions were not decreased by rosmarinic
601 acid. In addition, the regeneration of the rosmarinate radical by α-tocopherol was also
602 unlikely since this reaction was slow and α-tocopherol did not alter R0 degradation rates.
603 Instead α-tocopherol and R0 interactions produced an increase in antioxidant activity by
604 promoting the conversion of rosmarinic acid into caffeic acid thus providing a third molecule
605 that could inhibit lipid oxidation and increased the oxidative stability of the O/W emulsion. In
606 contrast, R12 in combination with α-tocopherol did not produce synergistic antioxidant
607 activity and did not significantly increase its conversion into caffeic acid during lipid

608 oxidation in O/W emulsions. This could be because R12 did not interact strongly with α-
609 tocopherol as determined by fluorescence. Overall, physical interaction between α-tocopherol
610 and rosmarinic acid or its alkyl esters seems to be an important factor in their ability to inhibit
611 lipid oxidation. Further research is needed to determine if physical interactions are important
612 in determining the antioxidant activity of combinations of other antioxidants.

613

614 **ACKNOWLEDGMENTS**

615 I would like to express my thanks to Prof. Dr. Paul M. Lahti at the chemistry department,
616 UMass Amherst for being a member of my committee. I appreciated for his donating valuable
617 times to teach and suggest me on developing EPR techniques used in this research.

618

BIBLIOGRAPHY

1. Gardner, H. W.; Kleiman, R.; Weisleder, D.; Inglett, G. E., Cysteine adds to lipid hydroperoxide. *Lipids* **1977,** 12, (8), 655-660.
2. Lambelet, P. S., F. and Loliger, J, Radical exchange reactions between vitamin E and vitamin C and phospholipids in autoxidizing polyunsaturated lipids. *Free Rad. Res* **1994,** 20, (1), 1-10.
3. Sims, R. J.; Fioriti, J. A., Methional as an antioxidant for vegetable-oils. *Journal of the American Oil Chemists Society* **1977,** 54, (1), 4-7.
4. Terao, J.; Yamauchi, R.; Murakami, H.; Matsushita, S., Inhibitory effects of tocopherols and beta-carotene on singlet oxygen-initiated photo-oxidation of methyl linoleate and soybean oil. *Journal of Food Processing and Preservation* **1980,** 4, (1-2), 79-93.
5. Burton, G. W.; Ingold, K. U., Beta-carotene - An unusual type of lipid antioxidant. *Science* **1984,** 224, (4649), 569-573.
6. Kennedy, T. A.; Liebler, D. C., Peroxyl radical scavenging by beta-carotene in lipid bilayers - effect of oxygen partial-pressure. *Journal of Biological Chemistry* **1992,** 267, (7), 4658-4663.
7. Palozza, P.; Krinsky, N. I., Beta-carotene and alpha-tocopherol are synergistic antioxidants. *Archives of Biochemistry and Biophysics* **1992,** 297, (1), 184-187.
8. Parker, T. L.; Miller, S. A.; Myers, L. E.; Miguez, F. E.; Engeseth, N. J., Evaluation of synergistic antioxidant potential of complex mixtures using oxygen radical absorbance capacity (ORAC) and electron paramagnetic resonance (EPR). *Journal of agricultural and food chemistry* **2010,** 58, (1), 209-17.
9. Freeman, B. L.; Eggett, D. L.; Parker, T. L., Synergistic and Antagonistic Interactions of Phenolic Compounds Found in Navel Oranges. *Journal of Food Science* **2010,** 75, (6), C570-C576.
10. Gonzalez, E. A.; Nazareno, M. A., Antiradical action of flavonoid-ascorbate mixtures. *Lwt-Food Science and Technology* **2011,** 44, (2), 558-564.
11. Liu, D. H.; Shi, J.; Ibarra, A. C.; Kakuda, Y.; Xue, S. J., The scavenging capacity and synergistic effects of lycopene, vitamin E, vitamin C, and beta-carotene mixtures on the DPPH free radical. *Lwt-Food Science and Technology* **2008,** 41, (7), 1344-1349.
12. Hidalgo, M.; Sanchez-Moreno, C.; de Pascual-Teresa, S., Flavonoid-flavonoid interaction and its effect on their antioxidant activity. *Food Chemistry* **2010,** 121, (3), 691-696.
13. Chen, J.; Shi, J.; Macnaughton, L.; Kakuda, Y.; Xue, S. J.; Ma, Y.; Zhang, M.; Jiang, Y., The scavenging capacity of combinations of lycopene, B-carotene, vitamin e, and vitamin c on the free radical 2,2-diphenyl-1-picrylhydrazyl (DPPH). *Journal of Food Biochemistry* **2009,** 33, (2), 232-245.
14. Hiramoto, K.; Miura, Y.; Ohuki, G.; Kato, T.; Kikigawa, K., Are water-soluble natural antioxidants: synergistic in combination with alpha-tocopherol. *Journal of oleo science* **2002,** 51, (9), 569-576.
15. Pedrielli, P.; Skibsted, L. H., Antioxidant synergy and regeneration effect of quercetin, (-)-epicatechin, and (+)-catechin on alpha-tocopherol in homogeneous solutions of peroxidating methyl linoleate. *Journal of agricultural and food chemistry* **2002,** 50, (24), 7138-7144.
16. Alamed, J.; Chaiyasit, W.; McClements, D. J.; Decker, E. A., Relationships between Free Radical Scavenging and Antioxidant Activity in Foods. *Journal of agricultural and food chemistry* **2009,** 57, (7), 2969-2976.
17. Fukuzawa, K.; Ikebata, W.; Sohmi, K., Location, antioxidant and recycling dynamics of alpha-tocopherol in liposome membranes. *Journal of Nutritional Science and Vitaminology* **1993,** 39, S9-S22.
18. Lecomte, J.; Giraldo, L. J. L.; Laguerre, M.; Baréa, B.; Villeneuve, P., Synthesis, characterization and free radical scavenging properties of rosmarinic acid fatty esters. *Journal of the American Oil Chemists' Society* **2010,** 87, (6), 615-620.
19. Waraho, T.; Cardenia, V.; Rodriguez-Estrada, M. T.; McClements, D. J.; Decker, E. A., Prooxidant mechanisms of free fatty acids in stripped soybean oil-in-water emulsions. *Journal of agricultural and food chemistry* **2009,** 57, (15), 7112-7.

20. Boon, C. S.; Xu, Z.; Yue, X.; McClements, D. J.; Weiss, J.; Decker, E. A., Factors affecting lycopene oxidation in oil-in-water emulsions. *Journal of agricultural and food chemistry* **2008,** 56, (4), 1408-1414.
21. Faraji, H.; McClements, D. J.; Decker, E. A., Role of continuous phase protein on the oxidative stability of fish oil-in-water emulsions. *Journal of agricultural and food chemistry* **2004,** 52, (14), 4558-4564.
22. Bligh, E. G.; Dyer, W. J., A rapid method of total lipid extraction and purification. *Canadian Journal of Biochemistry and Physiology* **1959,** 37, (8), 911-917.
23. Panya, A.; Laguerre, M.; Lecomte, J.; Villeneuve, P.; Weiss, J.; McClements, D. J.; Decker, E. A., Effects of chitosan and rosmarinate esters on the physical and oxidative stability of liposomes. *Journal of agricultural and food chemistry* **2010,** 58, (9), 5679-5684.
24. Fujimoto, A.; Masuda, T., Antioxidation mechanism of rosmarinic acid, identification of an unstable quinone derivative by the addition of odourless thiol. *Food Chemistry* **2012,** 132, (2), 901-906.
25. Wilson, G. J.; Lin, C. Y.; Webster, R. D., Significant differences in the electrochemical behavior of the α-, β-, γ-, and δ-tocopherols (Vitamin E). *The Journal of Physical Chemistry B* **2006,** 110, (23), 11540-11548.
26. Pazos, M.; Torres, J. L.; Andersen, M. L.; Skibsted, L. H.; Medina, I., Galloylated polyphenols efficiently reduce alpha-tocopherol radicals in a phospholipid model system composed of sodium dodecyl sulfate (SDS) micelles. *Journal of agricultural and food chemistry* **2009,** 57, (11), 5042-8.
27. Laguerre, M.; Lopez Giraldo, L. J.; Lecomte, J.; Figueroa-Espinoza, M. C.; Barea, B.; Weiss, J.; Decker, E. A.; Villeneuve, P., Relationship between hydrophobicity and antioxidant ability of "phenolipids" in emulsion: a parabolic effect of the chain length of rosmarinate esters. *Journal of agricultural and food chemistry* **2010,** 58, (5), 2869-76.
28. Panya, A.; Laguerre, M.; Bayrasy, C.; Lecomte, J.; Villeneuve, P.; McClements, D. J.; Decker, E. A., An Investigation of the Versatile Antioxidant Mechanisms of Action of Rosmarinate Alkyl Esters in Oil-in-Water Emulsions. *Journal of agricultural and food chemistry* **2012,** 60, (10), 2692-2700.
29. Laguerre, M.; Giraldo, L. J.; Lecomte, J.; Figueroa-Espinoza, M. C.; Barea, B.; Weiss, J.; Decker, E. A.; Villeneuve, P., Chain length affects antioxidant properties of chlorogenate esters in emulsion: the cutoff theory behind the polar paradox. *Journal of agricultural and food chemistry* **2009,** 57, (23), 11335-42.
30. Buettner, G. R., The pecking order of free-radicals and antioxidants - lipid-peroxidation, alpha-tocopherol, and ascorbate. *Archives of Biochemistry and Biophysics* **1993,** 300, (2), 535-543.
31. Hotta, H.; Ueda, M.; Nagano, S.; Tsujino, Y.; Koyama, J.; Osakai, T., Mechanistic study of the oxidation of caffeic acid by digital simulation of cyclic voltammograms. *Analytical biochemistry* **2002,** 303, (1), 66-72.
32. Yang, B.; Kotani, A.; Arai, K.; Kusu, F., Estimation of the antioxidant activities of flavonoids from their oxidation potentials. *Analytical Sciences* **2001,** 17, (5), 599-604.
33. Kilmartin, P. A.; Zou, H. L.; Waterhouse, A. L., A cyclic voltammetry method suitable for characterizing antioxidant properties of wine and wine phenolics. *Journal of agricultural and food chemistry* **2001,** 49, (4), 1957-1965.
34. Gunckel, S.; Santander, P.; Cordano, G.; Ferreira, J.; Munoz, S.; Nunez-Vergara, L. J.; Squella, J. A., Antioxidant activity of gallates: an electrochemical study in aqueous media. *Chemico-biological interactions* **1998,** 114, (1-2), 45-59.
35. Firuzi, O.; Lacanna, A.; Petrucci, R.; Marrosu, G.; Saso, L., Evaluation of the antioxidant activity of flavonoids by "ferric reducing antioxidant power" assay and cyclic voltammetry. *Biochimica Et Biophysica Acta-General Subjects* **2005,** 1721, (1-3), 174-184.
36. Simic, A.; Manojlovic, D.; Segan, D.; Todorovic, M., Electrochemical Behavior and antioxidant and prooxidant activity of natural phenolics. *Molecules* **2007,** 12, (10), 2327-2340.
37. Born, M.; Carrupt, P. A.; Zini, R.; Bree, F.; Tillement, J. P.; Hostettmann, K.; Testa, B., Electrochemical behaviour and antioxidant activity of some natural polyphenols. *Helvetica Chimica Acta* **1996,** 79, (4), 1147-1158.

722 38. Shahidi, F.; Zhong, Y., Revisiting the Polar Paradox Theory: A Critical Overview. *Journal of*
723 *agricultural and food chemistry* **2011,** 59, (8), 3499-3504.
724 39. Lopez-Giraldo, L. J.; Laguerre, M.; Lecomte, J.; Figueroa-Espinoza, M. C.; Barea, B.; Weiss, J.;
725 Decker, E. A.; Villeneuve, P., Kinetic and stoichiometry of the reaction of chlorogenic acid and its alkyl
726 esters against the DPPH radical. *Journal of agricultural and food chemistry* **2009,** 57, (3), 863-870.
727 40. Kikuzaki, H.; Nakatani, N., Structure of a new antioxidative phenolic acid from oregano
728 (origanum-vulgare L). *Agricultural and Biological Chemistry* **1989,** 53, (2), 519-524.
729 41. Nakazawa, T.; Ohsawa, K., Metabolism of rosmarinic acid in rats. *Journal of Natural Products*
730 **1998,** 61, (8), 993-996.
731 42. Bel-Rhlid, R.; Crespy, V.; Page-Zoerkler, N.; Nagy, K.; Raab, T.; Hansen, C. E., Hydrolysis of
732 Rosmarinic Acid from Rosemary Extract with Esterases and Lactobacillus johnsonii in Vitro and in a
733 Gastrointestinal Model. *Journal of agricultural and food chemistry* **2009,** 57, (17), 7700-7705.
734 43. Peyrat-Maillard, M. N.; Cuvelier, M. E.; Berset, C., Antioxidant activity of phenolic compounds
735 in 2,2 '-azobis (2-amidinopropane) dihydrochloride (AAPH)-induced oxidation: Synergistic and
736 antagonistic effects. *Journal of the American Oil Chemists Society* **2003,** 80, (10), 1007-1012.
737 44. Jung, D. M.; de Ropp, J. S.; Ebeler, S. E., Study of interactions between food phenolics and
738 aromatic flavors using one- and two-dimensional H-1 NMR spectroscopy. *Journal of agricultural and*
739 *food chemistry* **2000,** 48, (2), 407-412.
740 45. Maccarone, E.; Maccarrone, A.; Rapisarda, P., Stabilization of anthocyanins of blood orange
741 fruit juice. *Journal of Food Science* **1985,** 50, (4), 901-904.
742 46. Foley, S.; Navaratnam, S.; McGarvey, D. J.; Land, E. J.; Truscott, T. G.; Rice-Evans, C. A., Singlet
743 oxygen quenching and the redox properties of hydroxycinnamic acids. *Free Radical Biology and*
744 *Medicine* **1999,** 26, (9-10), 1202-1208.
745 47. Chen, J. H.; Ho, C. T., Antioxidant activities of caffeic acid and its related hydroxycinnamic
746 acid compounds. *Journal of agricultural and food chemistry* **1997,** 45, (7), 2374-2378.
747
748
749
750
751
752

753 **Figure list**

754

755 **Figure 1. Lipid** hydroperoxide (A) and hexanal (B) formation in 1% stripped soybean oil-
756 Tween 20 emulsions at 25$^{o}$C in the presence of individual of rosmarinic acid and its alkyl
757 esters and α-tocopherol (TOH) (30μM). Data points and error bars represent means (n=3) ±
758 standard deviations.

759 **Figure 2.** Lipid hydroperoxide (A) and hexanal (B) formation in 1 % stripped soybean oil-
760 Tween 20 emulsions at 25 $^{o}$C in the presence of combinations of rosmarinic acid and its alkyl
761 esters with α-tocopherol (TOH) (30 μM + 30 μM). Data points and error bars represent means
762 (n=3) ± standard deviations.

763 **Figure 3.** Interaction indexes of the combinations of rosmarinic acid and its esters with α-
764 tocopherol in 1% stripped soybean oil-Tween 20 emulsions at 25$^{o}$C. Data were calculated
765 from oxidation lag time obtained from lipid hydroperoxide and hexanal formation.

766 **Figure 4.** The antioxidant partitioning of rosmarinic acid (R0), butyl (R4), dodecyl (R12) and
767 eicosyl (R20) rosmarinate esters and α-tocopherol (100 μM) into aqueous phase of O/W
768 emulsions (not washed). Data points and error bars represent means (n=3) ± standard
769 deviations.

770 **Figure 5.** Fluorescence quenching of α-tocopherol ($\lambda_{em}$= 325 nm) by rosmarinic acid and
771 rosmarinate esters in O/W emulsions with/without influences of surfactant micelles.

772 **Figure 6.** Regeneration efficiencies of the rosmarinic acid esters to reduced α-tocopheroxyl
773 radicals in homogenous (ethanol) and heterogeneous (Tween 20) micelle solutions. Dash line
774 indicates ratios of regeneration efficiency of Tween 20 and ethanol. Data points and error bars
775 represent means (n=5) ± standard deviations.

**Figure 7.** Depletion of α-tocopherol (A), R0 (B), and R12 (C) when added individually at different concentrations (15, 30 and 60 μM) and their effect on hexanal formation during the oxidation of O/W emulsions at 25°C.

**Figure 8.** Depletion of rosmarinic acid (R0) and α-tocopherol (TOH) analyzed in combination and their effect on tocopherol quinone (TQ) and hexanal (Hex) formation in 1% stripped soybean oil-Tween 20 emulsions at 25°C. Three concentrations of R0 were tested (15, 30 and 60 μM) in combination with 30μM of α-tocopherol. Data points and error bars represent means (n = 3) ± standard deviations.

**Figure 9.** Depletion of rosmarinic acid (R12) and α-tocopherol (TOH) analyzed in combination and their effect on tocopherol quinone (TQ) and hexanal (Hex) formation in 1% stripped soybean oil-Tween 20 emulsions at 25°C. Three concentrations of R12 were tested (15, 30 and 60 μM) in combination with 30μM of α-tocopherol. Data points and error bars represent means (n = 3) ± standard deviations.

**Figure 10.** Structures of main antioxidant products observed during oxidation. A) represents reduced form of rosmarinic acid and dodecyl rosmarinate. B) represents the quinone formed on the 2-oxyphenylpropanyl moiety of dodecyl rosmarinate (the quinone of rosmarinic acid was not detected). C) represents caffeic acid observed in the oxidation of rosmarinic acid and dodecyl rosmarinate.1 EWIE: electron-withdrawing inductive effect

**Figure 11.** Accumulation ($A_{330}$) of caffeic acid (CA) in R0 (A) and R12 (B), and the quinone (RQ) in R12 (C) observed in the individual and the combinations with α-tocopherol at different concentrations during the oxidation in O/W emulsions.

800 **Table list**

801 **Table 1** Electrochemical parameters of tested antioxidants in acetonitrile, 50 mM phosphate
802 buffer (pH 7), and 1% Tween 20 in 50 mM phosphate buffer (pH 7) solutions at 25$^{o}$C
803 obtained from cyclic voltammetry (CV)

804

805

806

807

808

809

810

811

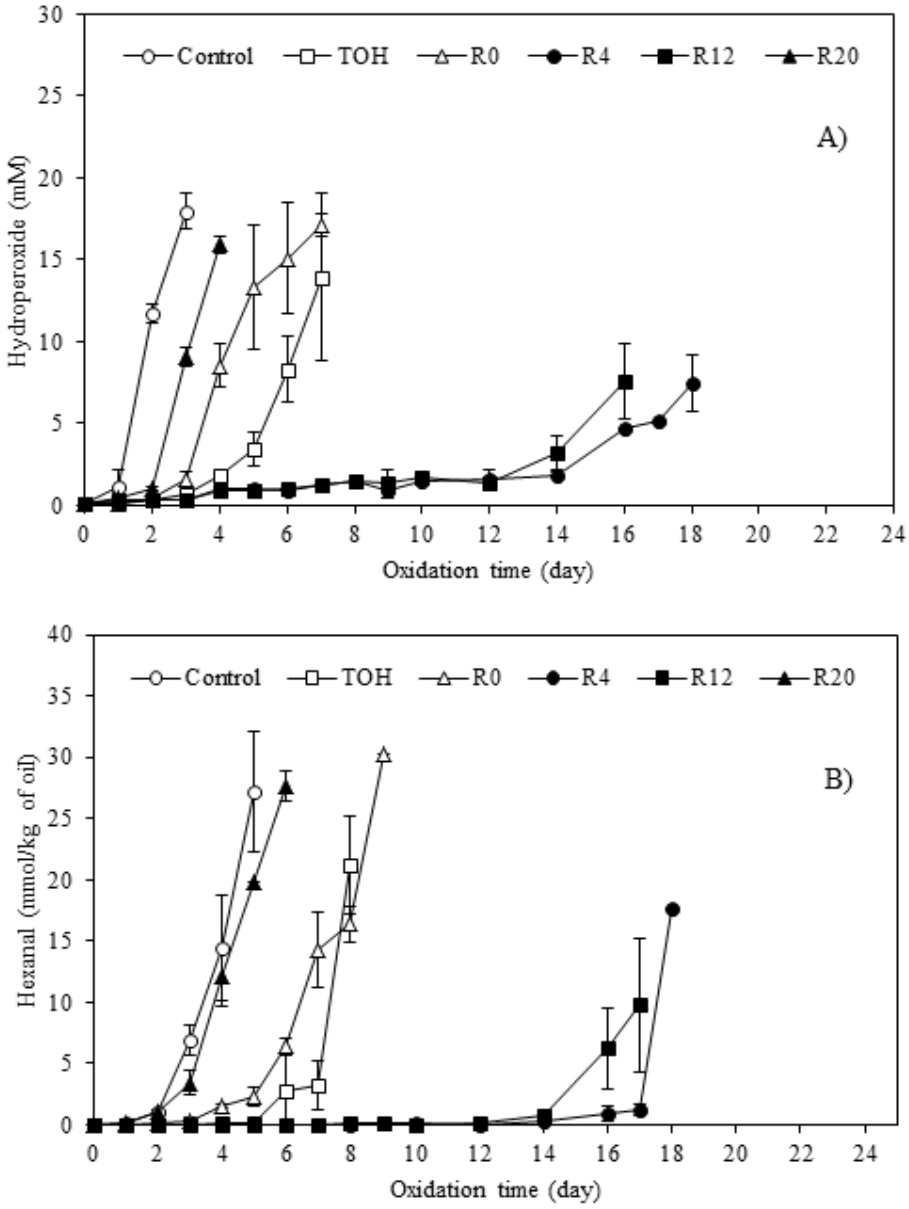
Control
TOH
R0
R4
R12
R20
A)
Hydroperoxide (mM)
Oxidation time (day)
B)
Hexanal (mmol/kg of oil)
Oxidation time (day)

**Figure 1.**

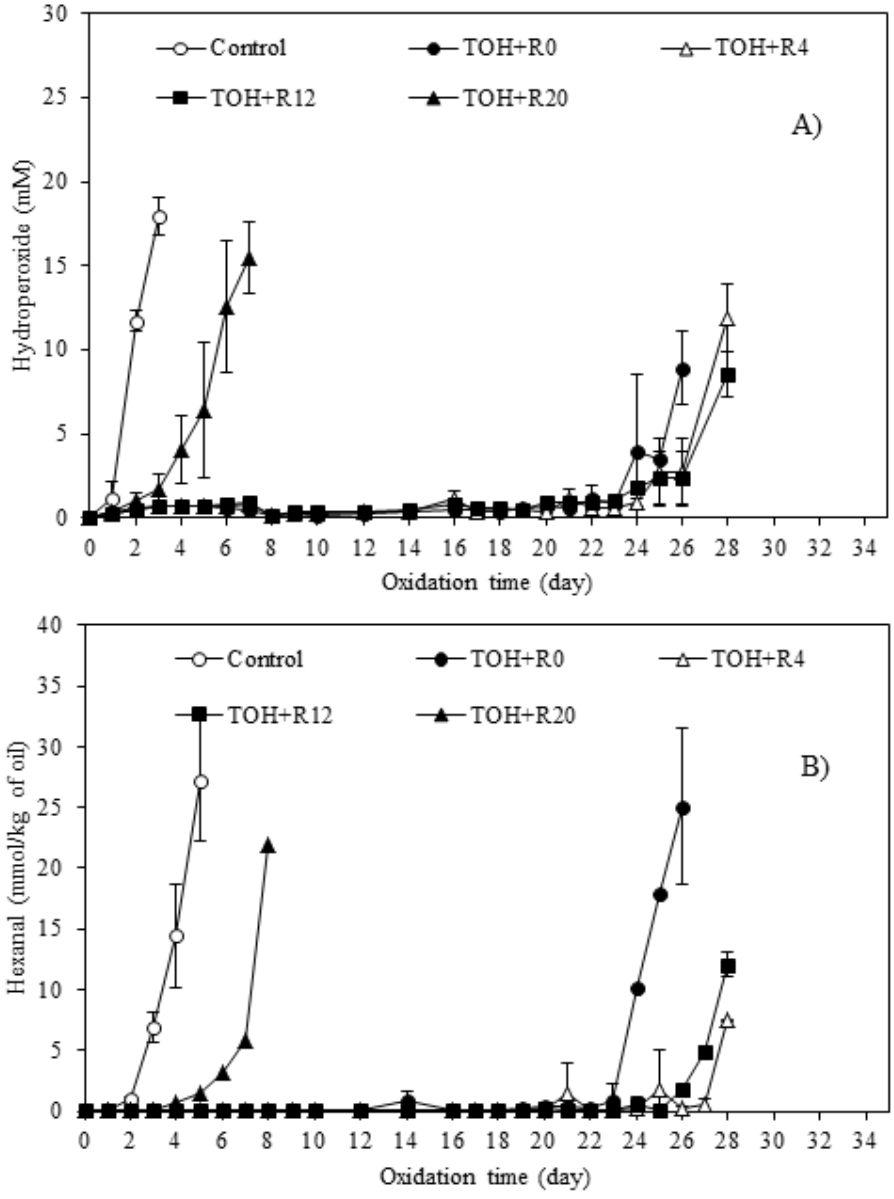
Control
TOH+R0
TOH+R4
TOH+R12
TOH+R20
A)
Hydroperoxide (mM)
Oxidation time (day)
B)
Hexanal (mmol/kg of oil)
Oxidation time (day)

**Figure 2.**

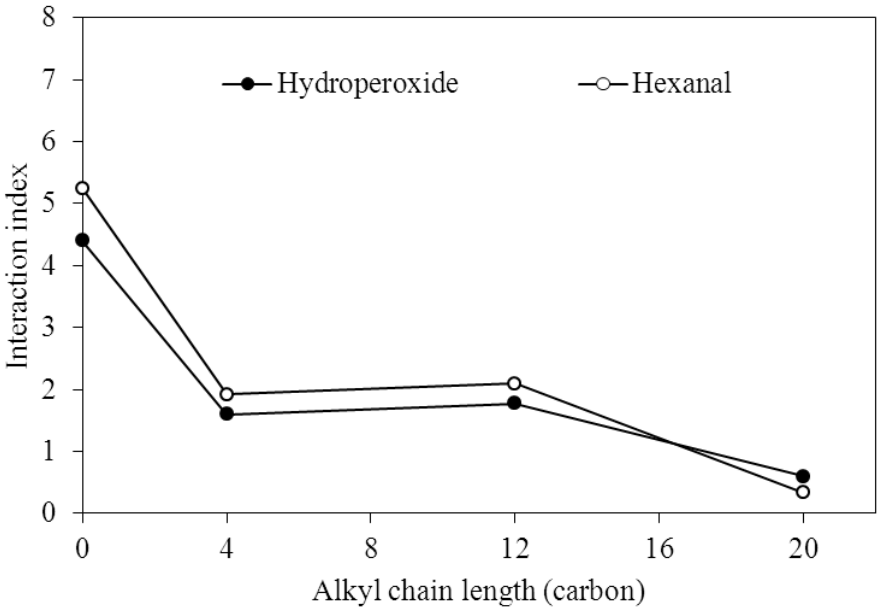
Hydroperoxide
Hexanal
Interaction index
Alkyl chain length (carbon)
0
1
2
3
4
5
6
7
8
0
4
8
12
16
20

**Figure 3.**

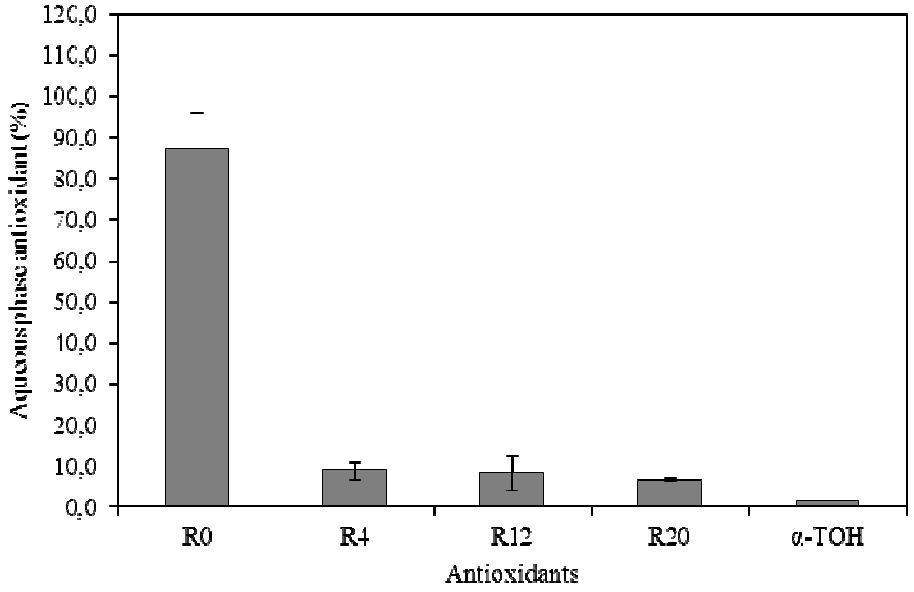
120,0
110,0
100,0
90,0
80,0
70,0
60,0
50,0
10,0
30,0
20,0
10,0
0,0
Aqueous phase antioxidant (%)
R0
R4
R12
R20
α-TOH
Antioxidants

**Figure 4.**

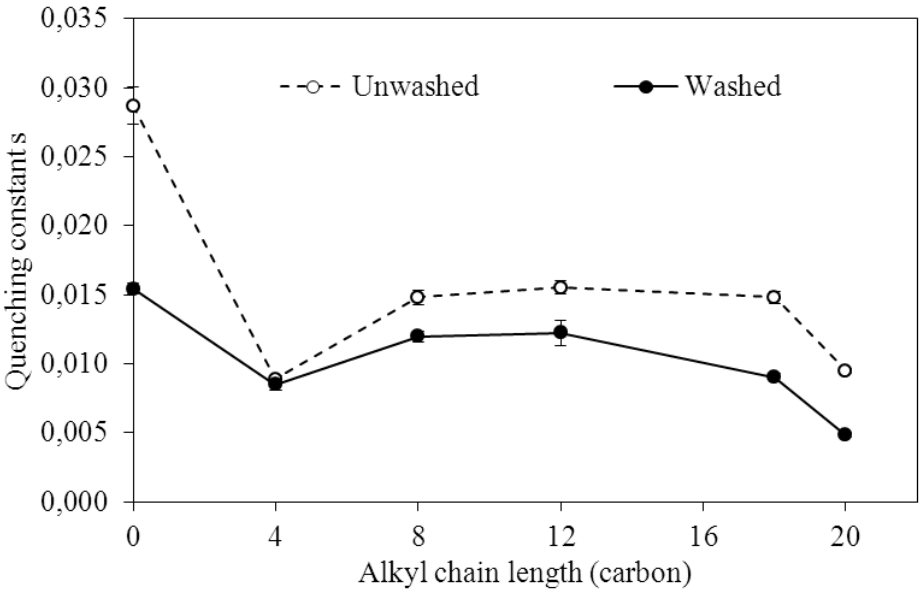
0,035
0,030
0,025
0,020
0,015
0,010
0,005
0,000
Quenching constant s
Unwashed
Washed
0
4
8
12
16
20
Alkyl chain length (carbon)

**Figure 5.**

875 **Table 1**

876

| Antioxidants | Oxidation peak potential (mV vs. Ag/AgCl) |
|---|---|
| R0 (ACN) | 1115.1±10.7 |
| R4 (ACN) | 1132.9±7.1 |
| R8 (ACN) | 1126.0±8.2 |
| R12 (ACN) | 1133.9±5.6 |
| R18 (ACN) | 1135.3±8.4 |
| R20 (ACN) | 1137.4±1.6 |
| α-TOH (ACN) | 634.9±0.85 |
| R0 (PBS, pH 7) | 359.0±19.2 |
| Trolox (PBS, pH 7) | 275.0±12.0 |
| R0 (Tw20, pH7) | 394.3±16.9 |
| α-TOH (Tw20, pH 7) | 263.3±2.3 |
| Trolox (Tw20, pH 7) | 298.7±18.5 |

877

878

879

880

881

882

883

884

885

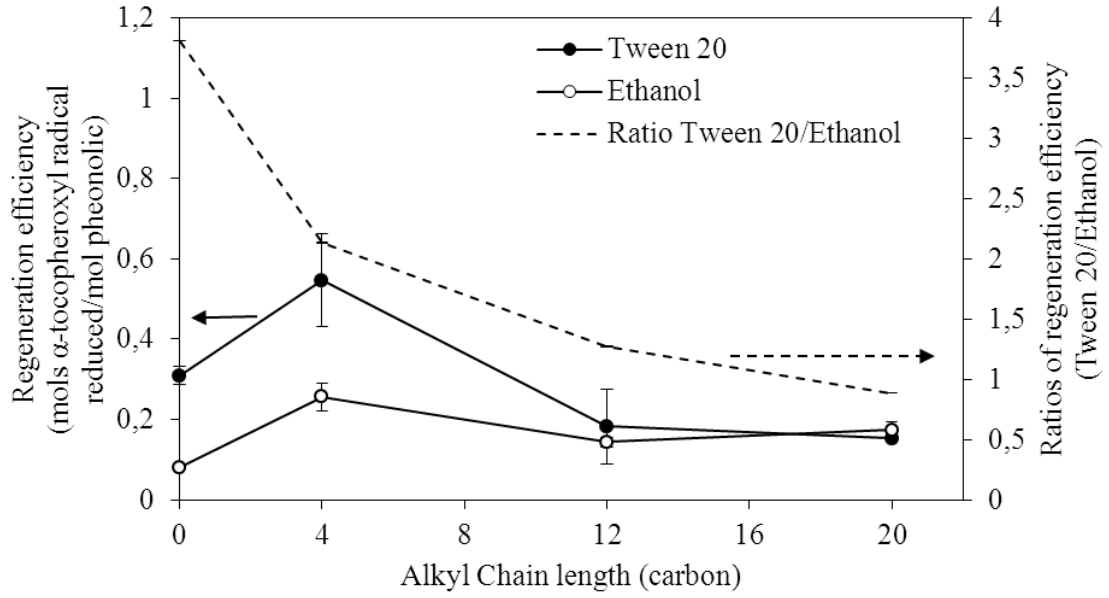
Tween 20
Ethanol
Ratio Tween 20/Ethanol
Regeneration efficiency (mols α-tocopheroxyl radical reduced/mol pheonolic)
Ratios of regeneration efficiency (Tween 20/Ethanol)
Alkyl Chain length (carbon)
0
0,2
0,4
0,6
0,8
1
1,2
0,5
1,5
2
2,5
3
3,5
4
4
8
12
16
20

**Figure 6.**

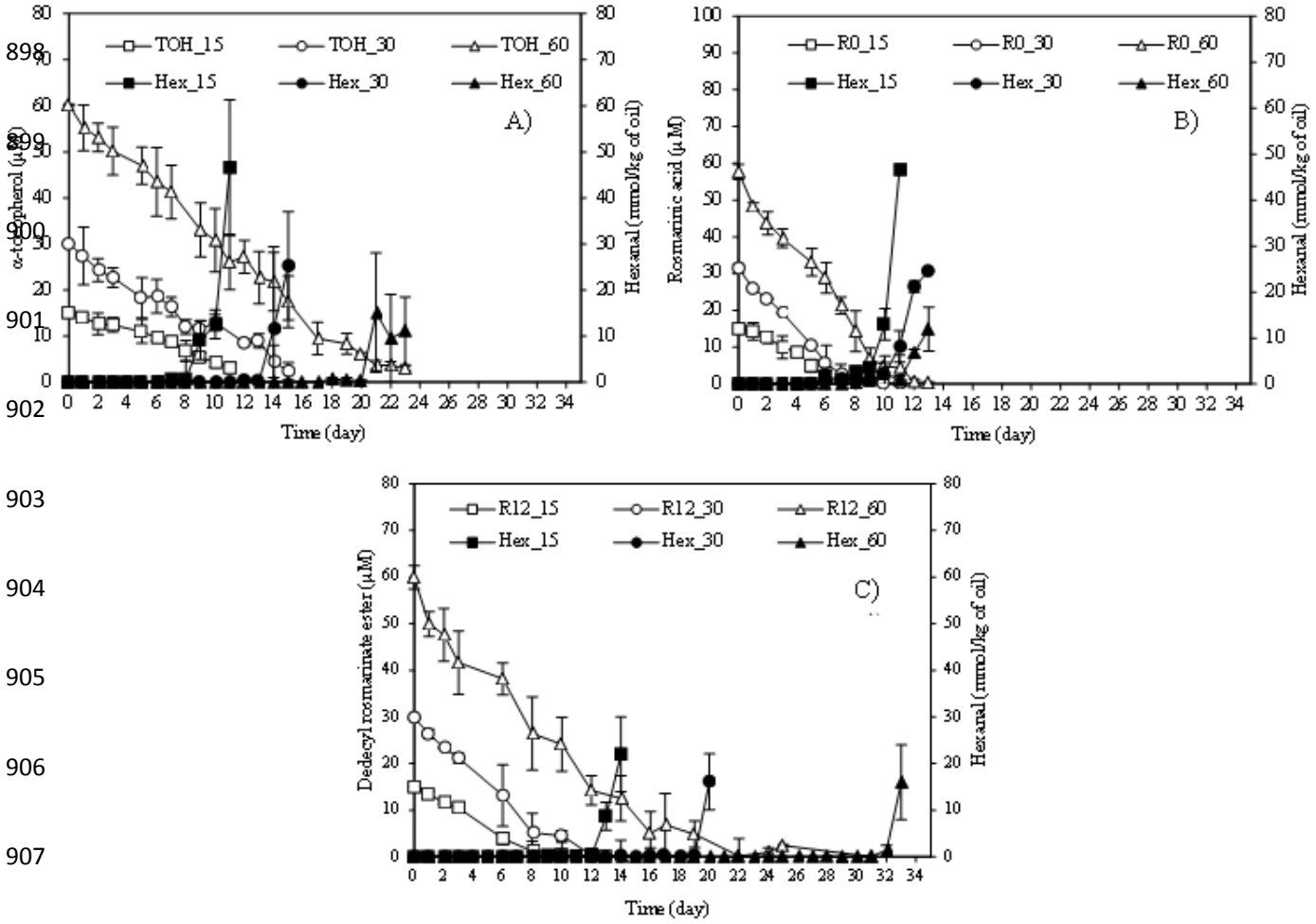
TOH_15
TOH_30
TOH_60
Hex_15
Hex_30
Hex_60
A)
α-tocopherol (μM)
Hexanal (mmol/kg of oil)
Time (day)
R0_15
R0_30
R0_60
Hex_15
Hex_30
Hex_60
B)
Rosmarinic acid (μM)
Hexanal (mmol/kg of oil)
Time (day)
R12_15
R12_30
R12_60
Hex_15
Hex_30
Hex_60
C)
Dedecyl rosmarinate ester (μM)
Hexanal (mmol/kg of oil)
Time (day)

**Figure 7.**

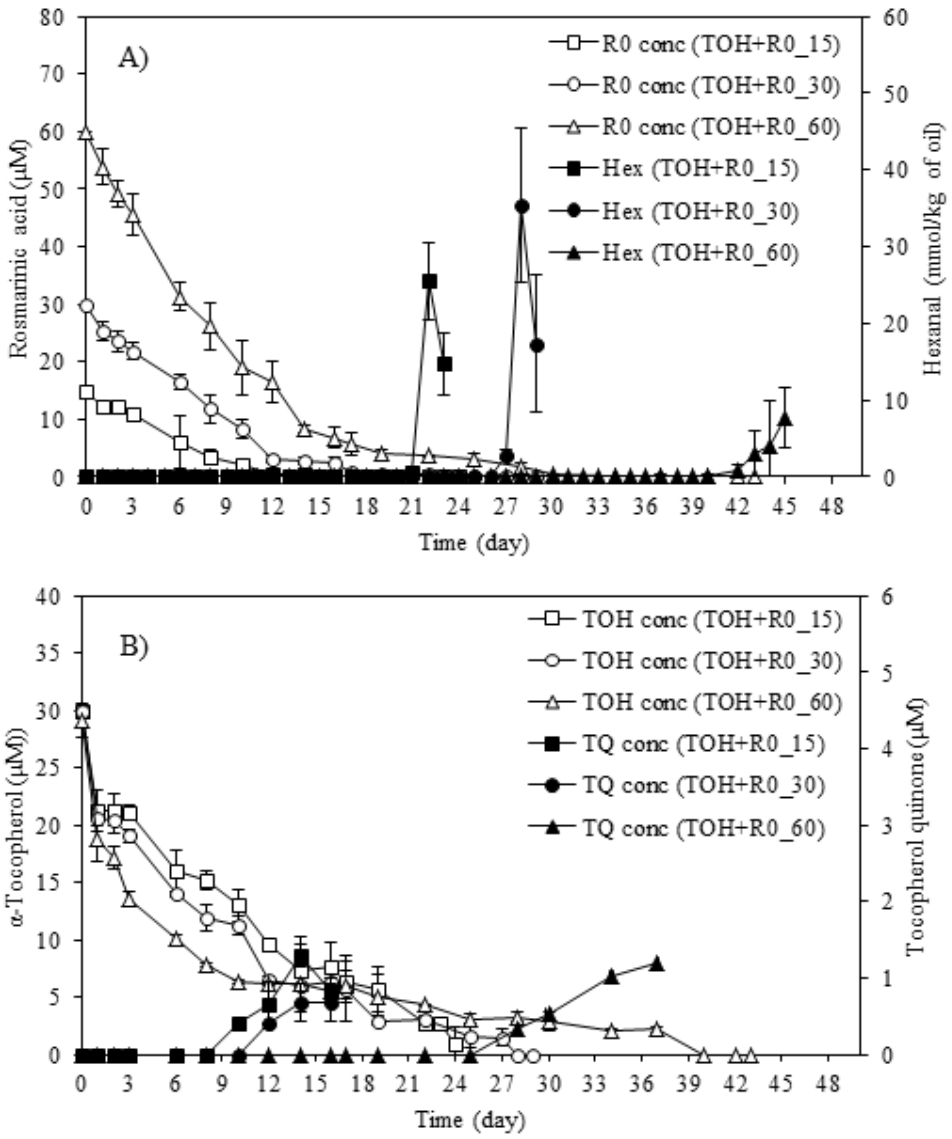
A)
R0 conc (TOH+R0_15)
R0 conc (TOH+R0_30)
R0 conc (TOH+R0_60)
Hex (TOH+R0_15)
Hex (TOH+R0_30)
Hex (TOH+R0_60)
Rosmarinic acid (μM)
Hexanal (mmol/kg of oil)
Time (day)
B)
TOH conc (TOH+R0_15)
TOH conc (TOH+R0_30)
TOH conc (TOH+R0_60)
TQ conc (TOH+R0_15)
TQ conc (TOH+R0_30)
TQ conc (TOH+R0_60)
α-Tocopherol (μM)
Tocopherol quinone (μM)
Time (day)

**Figure 8.**

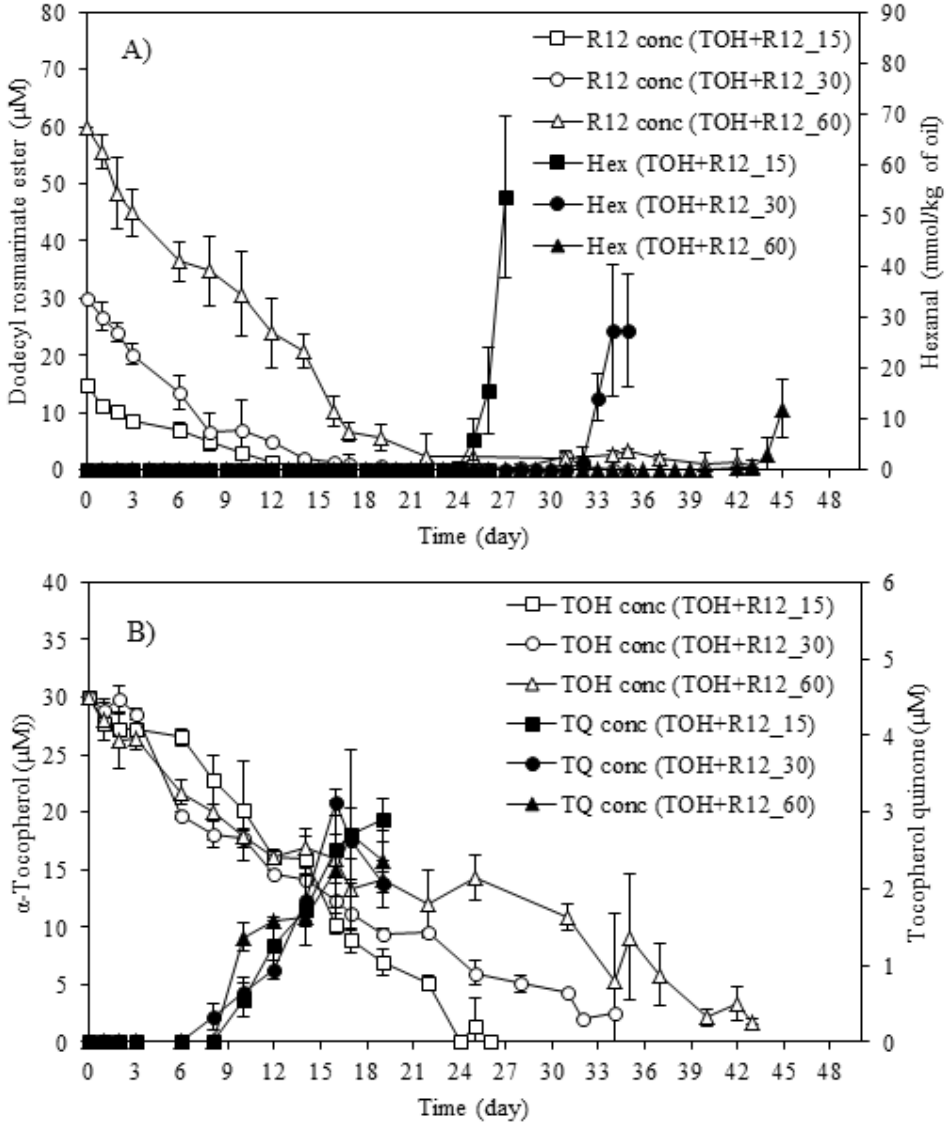
A)
R12 conc (TOH+R12_15)
R12 conc (TOH+R12_30)
R12 conc (TOH+R12_60)
Hex (TOH+R12_15)
Hex (TOH+R12_30)
Hex (TOH+R12_60)
Dodecyl rosmarinate ester (μM)
Hexanal (mmol/kg of oil)
Time (day)
B)
TOH conc (TOH+R12_15)
TOH conc (TOH+R12_30)
TOH conc (TOH+R12_60)
TQ conc (TOH+R12_15)
TQ conc (TOH+R12_30)
TQ conc (TOH+R12_60)
α-Tocopherol (μM)
Tocopherol quinone (μM)
Time (day)

**Figure 9.**

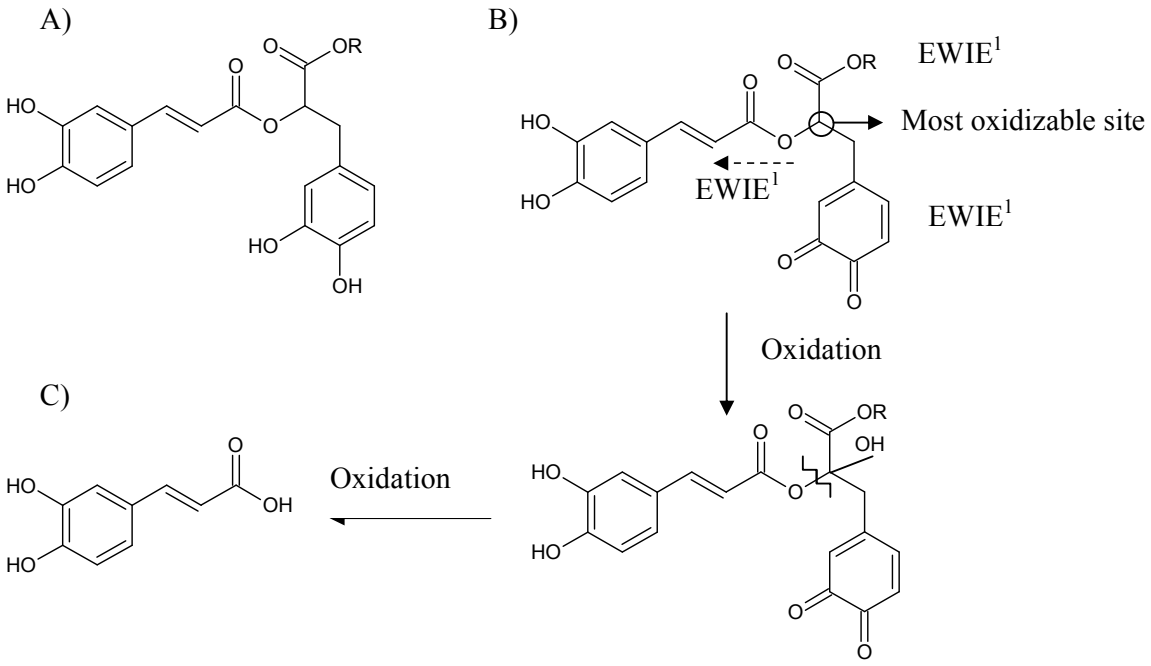


R = H , Rosmarinic acid; R= $C_{12}H_{25}$, Dodecyl rosmarinate

**Figure 10.**

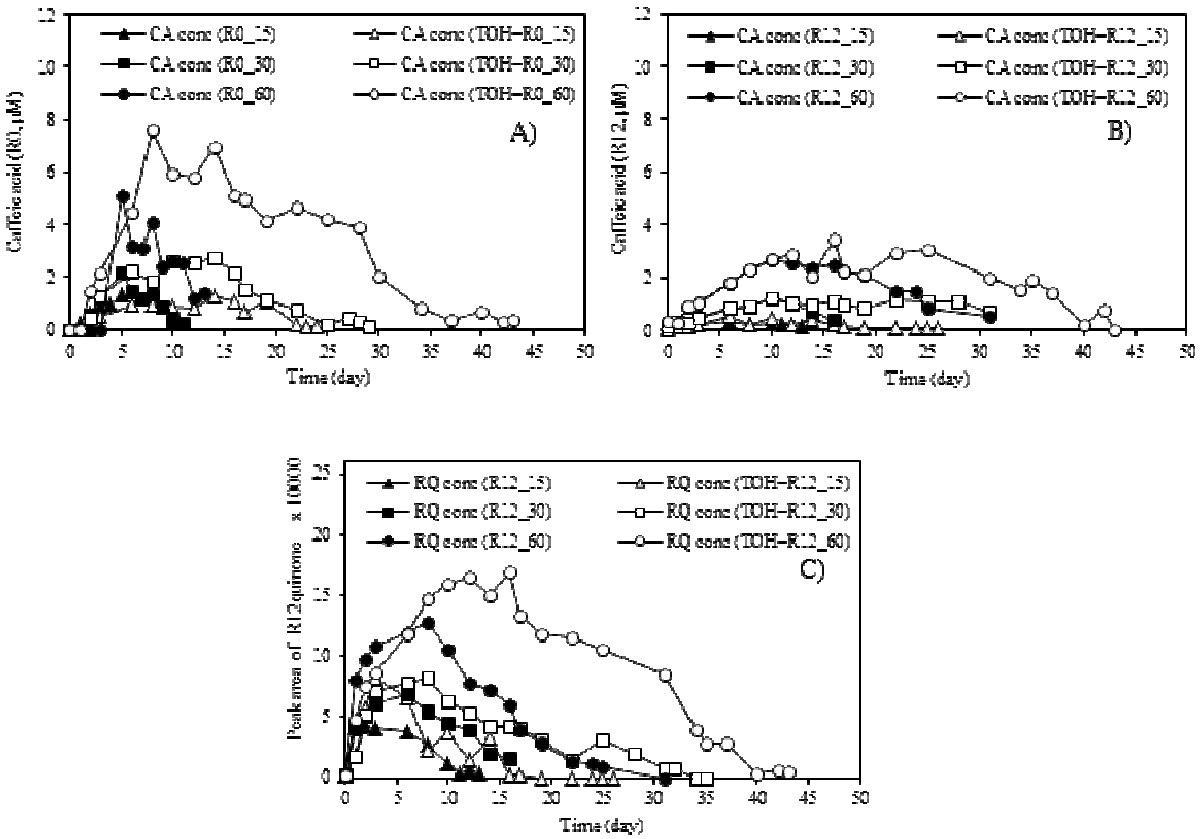
CA conc (R0_15)
CA conc (TOH-R0_15)
CA conc (R0_30)
CA conc (TOH-R0_30)
CA conc (R0_60)
CA conc (TOH-R0_60)
A)
Time (day)
CA conc (R12_15)
CA conc (TOH-R12_15)
CA conc (R12_30)
CA conc (TOH-R12_30)
CA conc (R12_60)
CA conc (TOH-R12_60)
B)
Time (day)
RQ conc (R12_15)
RQ conc (TOH-R12_15)
RQ conc (R12_30)
RQ conc (TOH-R12_30)
RQ conc (R12_60)
RQ conc (TOH-R12_60)
C)
Time (day)

**Figure 11.**

973 **TOC graphic**

974

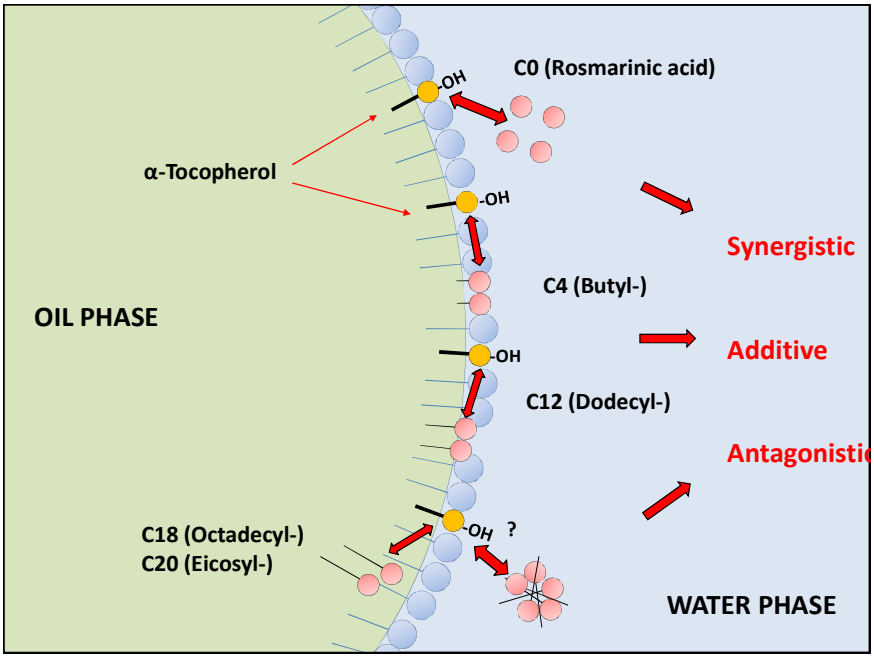


975

976

977

978

979

980

981

982

983

984

985

986

987

988